Osteoarthritis and Cartilage (2008) **16,** 1457–1465

doi:10.1016/j.joca.2008.04.006

Osteoarthritis and Cartilage

International Cartilage Repair Society

OARSI OSTEOARTHRITIS RESEARCH SOCIETY INTERNATIONAL

Chondrogenic differentiation of growth factor-stimulated precursor cells in cartilage repair tissue is associated with increased HIF-1α activity

K. Gelse M.D.†‡*, C. Mühle DiplBiochem§‖, K. Knaup Ph.D.§, B. Swoboda M.D.‡, M. Wiesener M.D., Ph.D.§, F. Hennig M.D.†, A. Olk M.D.† and H. Schneider M.D.§‖

† *Department of Trauma Surgery, University Hospital Erlangen, Germany*

‡ *Division of Orthopedic Rheumatology, University of Erlangen-Nuernberg, Germany*

§ *Interdisciplinary Center for Clinical Research, University Hospital Erlangen, Germany*

‖ *Department of Pediatrics, Medical University of Innsbruck, Austria*

Summary

Objective: To investigate the chondrogenic potential of growth factor-stimulated periosteal cells with respect to the activity of Hypoxia-inducible Factor 1α (HIF-1α).

Methods: Scaffold-bound autologous periosteal cells, which had been activated by Insulin-like Growth Factor 1 (IGF-1) or Bone Morphogenetic Protein 2 (BMP-2) gene transfer using both adeno-associated virus (AAV) and adenoviral (Ad) vectors, were applied to chondral lesions in the knee joints of miniature pigs. Six weeks after transplantation, the repair tissues were investigated for collagen type I and type II content as well as for HIF-1α expression. The functional role of phosphatidylinositol 3-kinase (PI3K)/mammalian target of rapamycin (mTOR) and mitogen-activated protein kinase (MEK)/extracellular signal-regulated kinase (ERK) signaling on BMP-2/IGF-1-induced HIF-1α expression was assessed *in vitro* by employing specific inhibitors.

Results: Unstimulated periosteal cells formed a fibrous extracellular matrix in the superficial zone and a fibrocartilaginous matrix in deep zones of the repair tissue. This zonal difference was reflected by the absence of HIF-1α staining in superficial areas, but moderate HIF-1α expression in deep zones. In contrast, Ad/AAVBMP-2-stimulated periosteal cells, and to a lesser degree Ad/AAVIGF-1-infected cells, adopted a chondrocyte-like phenotype with strong intracellular HIF-1α staining throughout all zones of the repair tissue and formed a hyaline-like matrix. *In vitro*, BMP-2 and IGF-1 supplementation increased HIF-1α protein levels in periosteal cells, which was based on posttranscriptional mechanisms rather than *de novo* mRNA synthesis, involving predominantly the MEK/ERK pathway.

Conclusion: This pilot experimental study on a relatively small number of animals indicated that chondrogenesis by precursor cells is facilitated in deeper hypoxic zones of cartilage repair tissue and is stimulated by growth factors which enhance HIF-1α activity.

Key words: Chondrogenesis, Cartilage repair, Hypoxia, HIF-1α, BMP-2, IGF-1.

Introduction

Chondral lesions of the joint surface have a limited endogenous healing potential because the access of repair cells to the lesions is restricted. Therefore, therapeutic attempts focus on the targeted supply of a cell population capable of producing new cartilage tissue. A number of mesenchymal tissues have been shown to contain cells with multilineage differentiation potential including chondrogenesis[1–5]. Cells from these donor tissues are available abundantly, can often be isolated by minimally invasive procedures without violating the articular surface, have a high proliferative capacity and retain their chondrogenic potential even in advanced age[6,7].

However, *in vitro* the differentiation of such precursor cells into chondrocyte-like cells hardly occurs spontaneously. Therefore, specific biochemical and biophysical stimuli including certain growth and differentiation factors, high cell densities or low oxygen levels are used to induce chondrogenesis. Within healthy articular cartilage tissue, chondrocytes are normally exposed to a hypoxic environment with oxygen levels as low as 1% in deep layers[8], and cell culture experiments have demonstrated that hypoxic conditions promote chondrogenesis and the synthesis of cartilage matrix components[9,10]. A central regulator of the adaptation of cells to low oxygen levels is the transcription factor Hypoxia-inducible Factor 1 (HIF-1), which is responsible for a variety of cellular functions including anaerobic energy supply, erythropoiesis, angiogenesis, regulation of the pH and cell survival[11–14]. Recent studies also suggested that its subunit HIF-1α plays an important role in chondrogenesis, joint formation and stabilization of the chondrocytic phenotype[12,15,16].

The regulation of HIF-1 levels is complex and the activity of this transcription factor is supposed to be predominantly modulated by the rate of specific protein degradation of its subunit HIF-1α rather than by stimulation of gene expression. Under physiological, normoxic conditions, oxygen-dependent prolyl hydroxylases (PHDs) modify two proline residues of the HIF-1α protein, which permits its recognition by the von Hippel-Lindau protein followed by capture through an E3-ubiquitin–ligase complex and subsequent

*Address correspondence and reprint requests to: Dr Kolja Gelse, Department of Trauma Surgery, University Hospital Erlangen, Krankenhausstr. 12, 91054 Erlangen, Germany. Tel: 49-9131-8223909; Fax: 49-9131-8533300; E-mail: kolja.gelse@web.de

Received 23 January 2008; revision accepted 19 April 2008.

rapid proteasomal degradation[14]. Among at least three HIF-specific PHDs1−3, which all might play distinct roles, PHD2 is considered as the key oxygen sensor controlling HIF-1α levels by catalyzing its degradation[17].

Here, we assessed the chondrogenic differentiation of unstimulated and Bone Morphogenetic Protein 2 (BMP-2)- or Insulin-like Growth Factor 1 (IGF-1)-stimulated, scaffold-bound periosteal cells that were applied to a large chondral lesion in miniature pigs. This study aimed at an evaluation of composition, quality and zonal pattern of the newly formed tissue with particular attention to the activity of HIF-1α. Furthermore, the functional relationship between IGF-1 or BMP-2 stimulation and HIF-1α activity and its mechanisms were of interest.

Materials and methods

ADENOVIRAL (Ad) AND ADENO-ASSOCIATED VIRUS (AAV) VECTORS

The Ad vectors AdBMP-2 and AdIGF-1, carrying human BMP-2 or IGF-1 cDNA, respectively, under the control of the CMV promotor, have been described[4]. Viruses were propagated in 911 cells, purified by ultracentrifugation in a caesium chloride gradient and dialyzed against a storage buffer containing 10% glycerol. The concentrations of the vector stocks, as determined by plaque assay on 911 cells, ranged from 1×10^{10} to 3×10^{10} plaque forming units (pfu)/ml.

The AAV serotype 2-derived vectors AAVBMP-2 and AAVIGF-1 were generated by inserting human BMP-2 or IGF-1 cDNA, respectively, under the control of a CMV promotor into an AAV type 2 backbone. Replication-deficient viruses were produced in human embryonic kidney (HEK293) cells by cotransfection of three plasmids as described by Xiao *et al.*[18] and purified according to established protocols[19]. The concentrations of the vector stocks ranged from 1.5×10^9 to 4.0×10^9 infectious particles (i.p.)/ml.

ISOLATION OF MESENCHYMAL CELLS

Six female adult miniature pigs aged 18 months (Ellegaard, Denmark) with body weights of 35−40 kg were used in this study.

For isolation of autologous periosteal cells, the pigs were anesthetized and cells were obtained from the cambium layer of the periosteum of the right tibia as described previously[20]. Cell culture was performed at 37°C, 5% CO_2, in Dulbecco's modified Eagle's medium (DMEM) supplemented with 10% fetal calf serum (FCS), insulin-transferrin-selenium (1× ITS) (Sigma-Aldrich, Munich, Germany), ascorbate-2-phosphate (50 μg/ml) and penicillin/streptomycin (100 units/ml). The cells were passaged after reaching confluence.

Characterization of the cell population included reverse transcription polymerase chain reaction (RT-PCR) to confirm a marker profile indicative of mesenchymal progenitor cells. Detection of CD13, CD34, CD45, CD90, Sca-1 and c-kit was done using the primer pairs listed in Table I.

IGF-1 AND BMP-2 GENE TRANSFER

Autologous periosteal cells were transferred into 15-cm dishes and, after reaching subconfluence, stimulated by BMP-2 or IGF-1 gene delivery (1.5×10^7 cells/dish). The vectors AdBMP-2 and AAVBMP-2, or AdIGF-1 and AAVIGF-1, were applied at predefined multiplicities of infection (MOI) of 100 pfu/cell and 1000 i.p./cell, respectively, to the cells in 10 ml of serum-free DMEM. Two hours after the infection, 10 ml of complete culture medium containing 20% FCS were added. Following incubation for another 24 h, the cells were washed with phosphate-buffered saline (PBS), mobilized using trypsin/ethylene diamine tetraacetic acid (EDTA), resuspended in DMEM containing 10% FCS and washed twice with this medium to remove non-internalized viral particles.

IN VITRO INFECTION AND QUANTIFICATION OF BMP-2 OR IGF-1 PRODUCTION

Periosteal cells were infected at subconfluence on 24-well plates (1×10^5 cells per well) either with AdBMP-2 or AdIGF-1 at 100 pfu/cell, AAVBMP-2 or AAVIGF-1 at 1000 i.p./cell or simultaneously with both the Ad and the AAV vector carrying the same growth factor DNA. The medium was replaced every 1−2 days and exactly 24 h before collecting the supernatant. Concentrations of IGF-1 and BMP-2 in cell supernatants were determined 4, 7, 14, 21 and 28 days following infection using commercially available enzyme-linked immunosorbent assay (ELISA) kits for BMP-2 (R&D Systems, Minneapolis, MN) and for IGF-1 (Diagnostics Systems Laboratories, Webster, TX), according to the manufacturers' protocols.

SCAFFOLD PREPARATION

Scaffolds were prepared as described previously[20]. Briefly, BMP-2-, IGF-1-stimulated or untreated periosteal cells were resuspended in 30 μl of fibrinogen (Beriplast, Aventis-Behring, Marburg, Germany) and seeded in a polyglycolic acid (PGA) matrix (Soft PGA Felt, Alpha Research, Berlin, Germany). Gel formation was achieved by adding 30 μl of thrombin solution (Beriplast, Aventis-Behring) to both sides of the cell-loaded scaffold, which was then incubated for another 48 h in culture medium to allow cell attachment.

SURGICAL PROCEDURES

Three weeks after periosteal cell isolation the animals were anesthetized as described previously[20]. Following disinfection of the skin around the left knee, the knee joint capsule was opened by a medial parapatellar incision, and the patella was displaced laterally. A large partial-thickness defect comprising the entire medial half of the articular surface of the patella was created using a custom-made planing tool in which the blade exceeds the basis by 0.6 mm. Since the thickness of miniature pig cartilage at this site is 0.7−0.9 mm, this device prevented injuries of the subchondral bone plate, which was confirmed by a complete absence of bleeding. The lateral half of the patella was left untreated and intact.

This cartilage defect was then treated by implantation of a cell-loaded PGA matrix. Two animals received a PGA scaffold containing 1.5×10^7 unstimulated autologous periosteal cells. In a second and third experimental groups ($n = 2$) scaffolds filled with 1.5×10^7 Ad/AAVIGF-1-infected or Ad/AAVBMP-2-infected autologous periosteal cells, respectively, were applied. The scaffold was fixed with two PGA pins (Resor-Pin, Geistlich Biomaterials, Wolhusen, Switzerland) as described previously[20]. To provide a smooth surface, a bilayer collagen membrane (Chondrogide; Geistlich Biomaterials, Wolhusen, Switzerland) was attached to the PGA matrix using a 5-0 polydioxanone suture. Then the patella was reduced and the stability of the graft was tested by repeated knee flexion. Joint capsule and skin were closed with vicryl sutures. The right knee joint, previously used for isolation of the periosteal cells, was left untreated.

After this procedure the animals were allowed to move freely in their cages and were sacrificed 6 weeks later. The animal study was approved by the appropriate Institutional and Governmental Review Boards.

HISTOLOGICAL AND IMMUNOHISTOCHEMICAL ASSESSMENT

The patella was fixed in 4% paraformaldehyde for at least 12 h, followed by decalcification in 0.5-M EDTA for 3 months. The large area of the repair tissue allowed the distinction between a proximal, an intermediate and a distal third of the patella, which were assessed separately. After standard processing in an automated tissue-processing machine, the samples were embedded in paraffin. Serial transverse 5-μm sections were cut and stained with toluidine blue to estimate the proteoglycan content or with hematoxylin and eosin for further histological investigation.

Immunohistochemical detection of type I and type II collagen was performed as described previously[20]. Briefly, deparaffinized sections were pretreated with 0.2% hyaluronidase (Roche, Mannheim, Germany) in PBS for 60 min and subsequently with pronase (2 mg/ml in PBS, pH 7.3; Sigma-Aldrich, Munich, Germany) for 60 min at 37°C. The sections were then left to react at 4°C with a monoclonal mouse anti-human type I collagen antibody (MP Biomedicals, Aurora, OH) diluted 1:200 or with a mouse anti-human type II collagen antibody (MP Biomedicals) diluted 1:500, followed by incubation with a biotinylated donkey anti-mouse secondary antibody (Dianova, Hamburg, Germany). Then a complex of streptavidin and biotinylated alkaline phosphatase was added. The sections were developed with fast red and counterstained with hematoxylin.

IMMUNOFLUORESCENCE

Serial sections of the patella were deparaffinized, pretreated with 10-mM Tris−HCl (pH 10) at 95°C for 5 min, followed by treatment with trypsin (Merck, Darmstadt, Germany) in PBS (1 mg/ml) at 37°C for 15 min. Unspecific antibody binding was blocked with 5% bovine serum albumin in PBS. The slides were incubated overnight at 4°C with a monoclonal mouse antibody against HIF-1α (Novus Biologicals, Littleton, CO) diluted in PBS at a ratio of 1:500. Specific binding was visualized by incubation with Cy3-conjugated goat anti-mouse secondary antibodies (Dianova) diluted 1:50 for 3 h. After washing with Tris buffered saline (TBS; 5 mM Tris in 0.9% NaCl, pH 7.35) the sections were covered with a mounting medium containing 4′-6′-Diamidino-2-phenylindole (Vector Inc., Peterborough, UK). Control slides were treated identically but without the Cy3-conjugated antibody. Three independent areas per specimen were investigated under a fluorescence microscope. The percentage of HIF-1α-positive cells per field of view was determined either in the superficial or in the deep half of the tissue.

Table I
Primer pairs used for specific gene analysis

Gene	Forward primer (5′–3′)	Reverse primer (5′–3′)
CD13	CTCCTCAGCGTTCGACTACC	CATCCTCCAGTTGTCCTCGT
CD34	GGCCAACGGAACAGAACTTA	CGACGGTTCATCAGCAAGTA
CD45	TGACCACTTCAGCAAGCATT	TGGAGCATCTTTGCACAGTC
CD90	AGAAGGTGACCAGCCTAACGG	TCTGAGCACTGTGACGTTCTG
Sca-1	TATGGTTTTGTGATGTTTGTCC	TAGATCCAGGGGCATTGTAG
c-Kit	GATGCCTTCAAGGATTTGGA	TCTGAGCACTGTGACGTTCTG
HIF-1α	AGGAATTATTTAGCATGTAGACTGCTGG	CATAACTGGTCAGCTGTGGTAATCC
PHD2	TCAATGGCCGGACGAAAG	CATTTGGATTATCAACATGACGTACA
B2M	GTCCCCCGAAGGTTCAGGT	AGGTCTGACTGCTCCGCG

TREATMENT OF PERIOSTEAL CELLS WITH RECOMBINANT BMP-2 OR IGF-1 AND INHIBITORS OF THE PI3K/mTOR AND MEK/ERK PATHWAY

Periosteal cells (second or third passage) which had been plated at a density of 5×10^5 cells/cm^2 were serum-starved for 12 h, followed by stimulation with recombinant human (rh) BMP-2 (R&D Systems, Minneapolis, MN) or rhIGF-1 (R&D Systems), respectively, at concentrations of 20 ng/ml or 100 ng/ml in serum-free medium for 24 h. A portion of the cells was treated simultaneously with Rapamycin (100 nM; Calbiochem, San Diego, CA), Wortmannin (100 nM; Calbiochem, San Diego, CA) or UO126 (10 μM; Promega, Madison, WI), respectively, for the same length of time. The experiment was performed in triplicates with cells from three different animals.

RNA ISOLATION AND RT-PCR

Total RNA was isolated from the cells with the Nucleo-Spin-RNA-II-Kit (Clontech Laboratories, Mountain View, CA). RNA yields were calculated by measuring the extinction at 260 nm. The reverse transcription reaction was performed using the First Strand cDNA synthesis kit (Roche, Mannheim, Germany). For detection of HIF-1α, PHD2 and the β2-microglobulin (B2M) housekeeping gene, the primer pairs listed in Table I were used. Each sample was subjected to 35 PCR cycles. PCR products were analyzed by gel electrophoresis on a 2.5% agarose gel.

IMMUNOBLOT ANALYSIS

Periosteal cells from individual animals were plated in six-well plates at a density of 5×10^5 cells/cm^2 and stimulated with rhBMP-2 or rhIGF-1 as described above. Nuclear and whole cell protein extracts were obtained from cultured cells as described previously[21]. PHD2, HIF-1α and α-tubulin were detected by Western immunoblot analysis using a polyclonal rabbit anti-PHD2 antibody diluted 1:1000 (Novus, Littleton, CO), a polyclonal rabbit anti-HIF-1α antibody diluted 1:200 (Cayman, Ann Arbor, MI) and a monoclonal rat anti-α-tubulin antibody diluted 1:1000 (AbD Serotec, Düsseldorf, Germany), respectively.

Nuclear extracts (50 μg/well) for the detection of HIF-1α or whole cell extracts (50 μg/well) for the detection of PHD2 and α-tubulin were separated on a 10% or 15% SDS-PAGE gel, respectively, and subsequently transferred to a nitrocellulose membrane (0.2 μm). The blots were blocked with 1% Western blocking reagent (Roche, Mannheim, Germany) overnight at 4°C and then probed with the specific antibodies for 4 h at room temperature. After washing with Tris buffered saline (TBS)-Tween, the blots were incubated with the respective secondary antibodies for 2 h. Bound antibodies were detected using BM chemiluminescence blotting substrate (peroxidase) (Roche, Mannheim, Germany).

STATISTICAL ANALYSIS

Data from the quantification of HIF-1α-positive cells were analyzed using Student's *t* test. *P* values below 0.01 were considered to be significant.

Results

PHENOTYPE OF THE PERICHONDRIAL CELLS USED

Basic characterization of cultured miniature pig periosteal cells by RT-PCR revealed the expression of stem cell-related antigens including Sca-1, CD13 and CD90, but no expression of c-Kit, CD34 or CD45, which indicates their mesenchymal progenitor status (data not shown).

Periosteal cells infected simultaneously with AdBMP-2 and AAVBMP-2 or AdIGF-1 and AAVIGF-1 produced BMP-2 or IGF-1, respectively, at biologically relevant levels during the entire detection period *in vitro*. After 4 weeks of culture, 1×10^5 cells still secreted significant levels of BMP-2 (13.8 ± 1.7 ng/24 h) or IGF-1 (14.2 ± 5.0 ng/24 h). AdBMP-2 infection alone led to high initial transgene expression with a rapid decline. In contrast, periosteal cells that had been infected with AAVBMP-2 alone showed sustained, but only low-level transgene expression (Fig. 1).

HISTOLOGICAL CHARACTERIZATION OF CARTILAGE REPAIR TISSUES AND DETECTION OF INTRACELLULAR HIF-1α ACTIVITY

The chondrogenic potential of BMP-2- or IGF-1-stimulated periosteal cells was investigated in a miniature pig model with a large partial-thickness cartilage defect comprising the medial half of the articular surface of the patella.

In six miniature pigs, autologous periosteal cells were obtained 3 weeks prior to surgical treatment and first expanded *ex vivo*. For two animals, a chondrogenic stimulus was then provided to the cells by Ad/AAV-mediated BMP-2 gene transfer, while cells of two other animals were infected with Ad/AAVIGF-1, followed by seeding into a bioresorbable scaffold and transplantation onto fresh chondral defects (Fig. 2). In another two animals, implants of unstimulated periosteal cells served as controls.

Six weeks after transplantation the cell-based grafts had integrated well into the preexisting cartilage in all animals and had resisted joint loading. Due to the thickness of the transplanted matrix, the height of the repair tissue exceeded

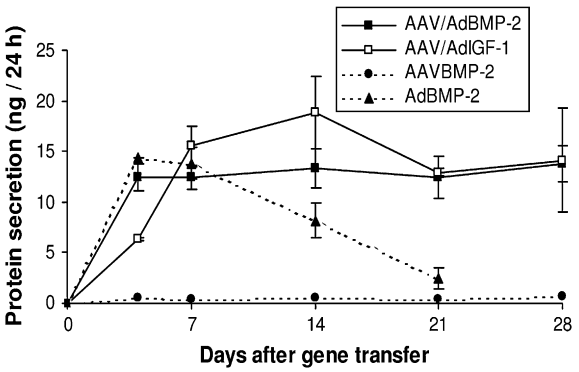

Fig. 1. Production of BMP-2 or IGF-1 by 1×10^5 porcine periosteal cells infected with AdBMP-2 or AdIGF-1 (100 pfu/cell) and/or AAVBMP-2 or AAVIGF-1 (1000 i.p./cell), respectively. The protein concentrations in the supernatant were determined with ELISAs. The daily protein secretion per ml medium is shown.

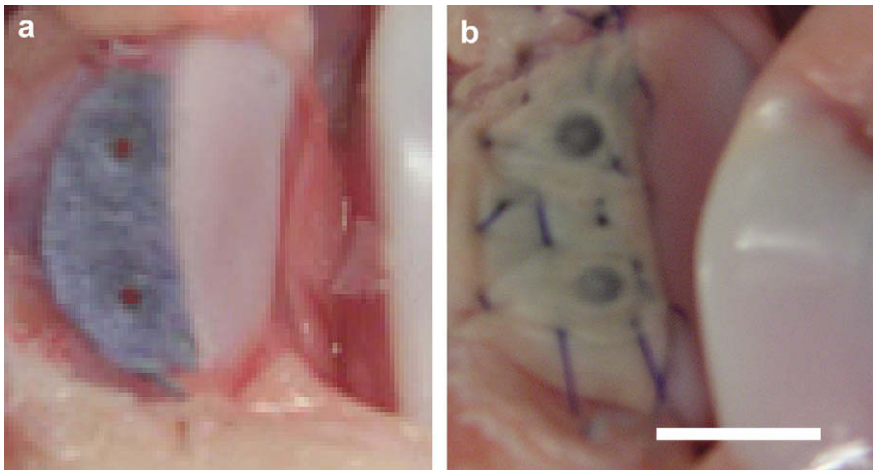

Fig. 2. Experimental model. In miniature pigs, partial-thickness chondral defects comprising the entire medial half of the articular surface of the patella were created using a custom-made planer. A cell-loaded PGA matrix was fixed with resorbable pins to the underlying bone (a). The upper part of the pin holes was milled out to allow lowering of the pin heads in plane with the surface. To create a smooth surface, an additional collagen membrane was sutured onto the PGA matrix (b). Bar = 1 cm.

that of adjacent cartilage in all six animals, and it showed some irregularities in the transitional area of the defect border [Fig. 3(a, b, f, g, k, l)]. The proteoglycan content of the newly formed tissue was assessed by toluidine blue staining. Parallel sections were additionally investigated by immunohistochemistry for type I collagen, a marker of bone and fibrous tissue, and type II collagen, a major and specific component of hyaline cartilage. Transplantation of unstimulated periosteal cells failed to generate hyaline cartilage [Figs. 3(a–e) and 4(b)]. The superficial half of the repair tissue showed virtually no proteoglycan and type II collagen staining and appeared to consist only of fibrous tissue. This notion was supported by the typical spindle-cell phenotype in the superficial and intermediate layers [Fig. 4(b)]. Deeper layers showed at best the formation of fibrocartilage, in which the cells partially adopted a round phenotype and formed a matrix with faint proteoglycan staining and partial type II collagen staining only in the deepest zone adjacent to the preexisting underlying cartilage. HIF-1α immunostaining was absent in almost all cells of the superficial half of the tissue, whereas approximately 40% of the cells in the deep zones of the tissue showed faint HIF-1α staining [Fig. 4(b), Table II].

The transplantation of Ad/AAVIGF-1-stimulated cells also failed to produce homogeneous hyaline repair tissue. Similar to the tissue formed by unstimulated cells, a fibrous superficial zone lacking type II collagen could be distinguished from fibrocartilaginous deeper zones. Only the latter were characterized by weak to moderate pericellular accumulation of proteoglycans and by a type II collagen-positive matrix [Fig. 3(f–j)]. Compared with the transplantation of unstimulated cells, there was an increase in cellularity both in the superficial and the deep zones, however, the morphological features of Ad/AAV-stimulated cells still differed from those of typical chondrocytes [Fig. 4(c)].

In contrast, repair tissue formed by Ad/AAVBMP-2-stimulated cells showed an intense staining for type II collagen throughout all layers with strong toluidine blue staining indicating a proteoglycan-rich matrix [Fig. 3(k–o)]. Most cells had adopted a chondrocyte-like round phenotype, but did not show the typical columnar distribution as observed in healthy articular cartilage. Occasionally, remnants of the PGA matrix were still detectable in the dense matrix. Interestingly, Ad/AAVBMP-2-stimulated cells were characterized by strong HIF-1α expression throughout the thickness of the cartilaginous repair tissue, and even in the superficial zone intracellular HIF-1α staining was clearly detectable in more than half of the cells [Fig. 4(d), Table II].

Articular cartilage from healthy, untreated joints served as an internal control. Here, the arrangement of the cells was zone-specific with a horizontal pattern in the most superficial layer and a perpendicular pattern in deep zones. Almost all chondrocytes in the deep zones displayed strong intracellular HIF-1α immunostaining with a continuous decrease toward the surface [Fig. 4(a), Table II].

In all samples analyzed, the underlying bone showed strong type I collagen staining and served as additional internal staining control. Type II collagen was always clearly detectable in intact hyaline cartilage and calcified cartilage.

INDUCTION OF HIF-1α EXPRESSION BY RECOMBINANT BMP-2 AND IGF-1 IS BASED ON POSTTRANSCRIPTIONAL MECHANISMS MEDIATED PREDOMINANTLY BY MEK/ERK SIGNALING

To investigate the mechanisms leading to elevated HIF-1α levels *in vivo*, periosteal cells were cultured in monolayers and exposed to rhBMP-2 or rhIGF-1 at concentrations of 20 or 100 ng/ml for 24 h. Under 21% oxygen, even the lower dose of rhBMP-2 (20 ng/ml) resulted in a distinct increase of intranuclear HIF-1α levels [Fig. 5(a)]. Stimulation with rhIGF-1 also yielded elevated HIF-1α levels. This effect was dose-dependent, and a distinct increase was only apparent at higher concentrations of IGF-1 (100 ng/ml). Thus, BMP-2 was more potent in this respect. *In vivo*, however, cells modified by Ad/AAV-mediated gene transfer may provide growth factor levels in the range of up to 10 ng/ml for at least 4 weeks (Fig. 1), but may not provide the high concentration (100 ng/ml) used in the stimulation experiments *in vitro*. As a positive control, periosteal cells cultured under 1% oxygen showed high intranuclear HIF-1α levels [Fig. 5(a)].

The next step was to investigate the mechanisms by which growth factors such as BMP-2 and IGF-1 lead to increased HIF-1α levels. The transcription factor HIF-1α is strongly regulated by the rate of specific protein degradation, and an important step in this rapid process is the

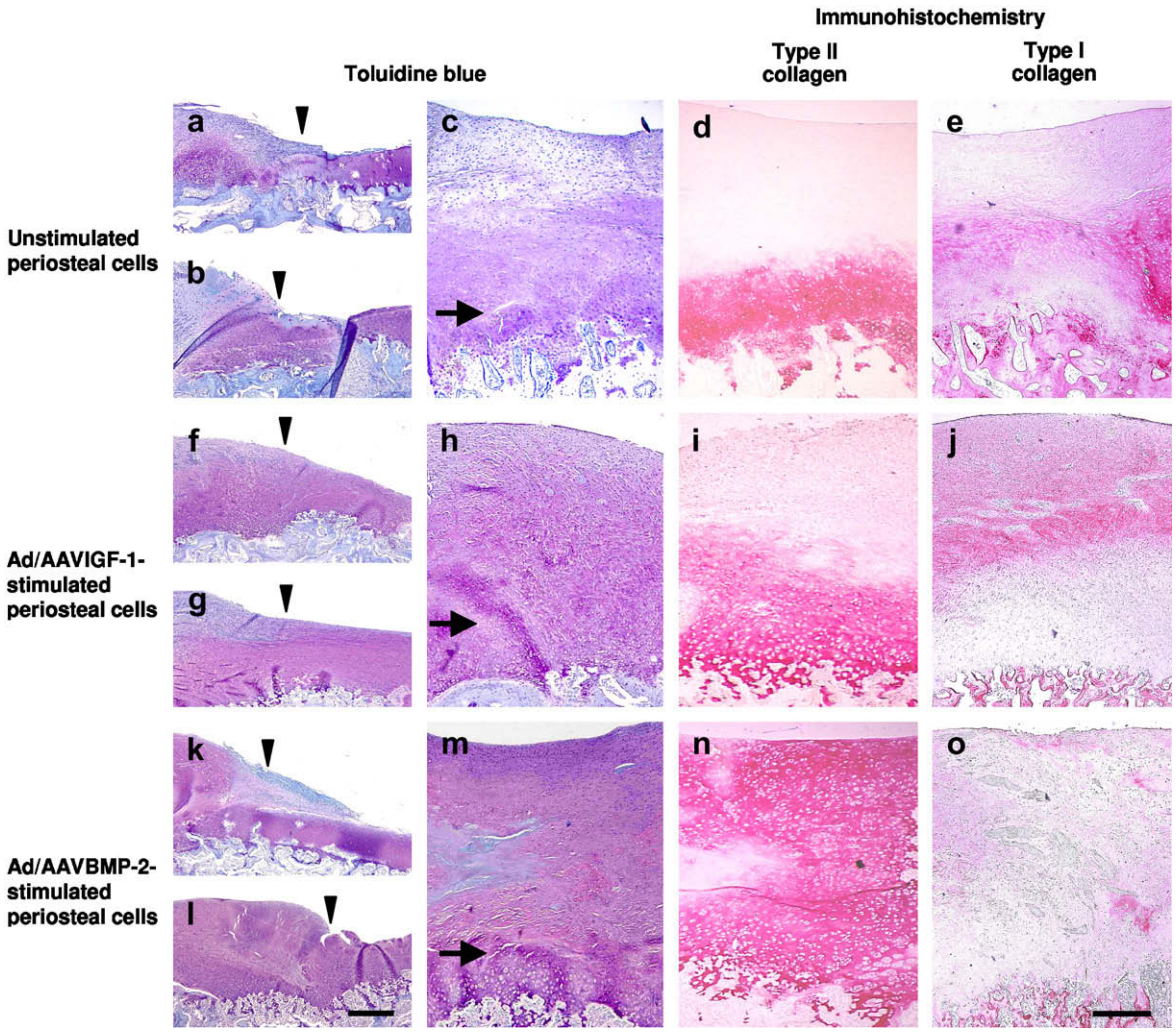

Fig. 3. Periosteal cell-based resurfacing of large cartilage lesions in miniature pigs. The cartilage defects were treated by implantation of a PGA matrix loaded with autologous periosteal cells. The resulting repair tissues were examined 6 weeks after cell transplantation by toluidine blue staining (a–c, f–h, k–m). In all six animals, the thickness of the repair tissue exceeded that of adjacent cartilage and showed some irregularities in the transitional area of the defect border (arrowheads in a, b, f, g, k, l). The repair tissue merged well with the underlying cartilage of the chondral lesions (arrows in c, h, m). Representative parallel sections were additionally evaluated by immunohistochemistry for type I and type II collagens. The underlying bone showed strong type I collagen staining (c, f, i) and served as internal control. Type II collagen was always clearly detectable in intact hyaline articular cartilage and calcified cartilage (b, e, h). Unstimulated cells formed fibrous repair tissue in superficial and middle zones which were positive for type I collagen (c), but negative for type II collagen (b). Only the deepest zone consisted of fibrocartilaginous tissue partially positive for type II collagen (b). Transplantation of Ad/AAVIGF-1-stimulated cells resulted in a fibrous superficial zone with strong staining for type I collagen (d, f), that could be distinguished from fibrocartilaginous deeper zones with moderate pericellular accumulation of proteoglycans and a type II collagen-positive matrix (d, e). In contrast, the repair tissue produced by Ad/AAVBMP-2-infected cells showed strong proteoglycan and type II collagen staining throughout all layers (g, h, i). Bar = 200 μm in c–e, h–j, m–o; Bar = 400 μm in a, b, f, g, k, l.

hydroxylation of HIF-1α at certain proline residues which is predominantly catalyzed by the oxygen-dependent hydroxylase PHD2. Neither rhBMP-2 nor rhIGF-1 had detectable influence on the intracellular level of PHD2 protein [Fig. 5(a)] or the expression of the PHD2 gene [Fig. 5(b)]. Cultivation under 1% oxygen had no effect on PHD2 protein or mRNA levels either [Fig. 5(a) and (b)]. Expression of HIF-1α was neither influenced by stimulation with IGF-1 or BMP-2 nor by hypoxia [Fig. 5(b)].

To investigate further the functional relationship between the growth factors and HIF-1α, we exposed IGF-1- and BMP-2-stimulated cells to inhibitors of the PI3K/mTOR or the MEK/ERK pathway. Application of Wortmannin or Rapamycin, inhibiting PI3K or mTOR, respectively, only moderately decreased the HIF-1α levels following BMP-2 and IGF-1 stimulation. However, treatment with the MEK inhibitor UO126 nearly completely abolished HIF-1α induction by either growth factor [Fig. 5(c)], indicating that this induction is based on posttranscriptional mechanisms mediated predominantly by MEK/ERK signaling.

Discussion

Biopsies of cartilage repair tissues resulting from microfracturing or autologous chondrocyte implantation often reveal zone-specific cellular differentiation patterns which are characterized by a superficial fibrous layer and areas

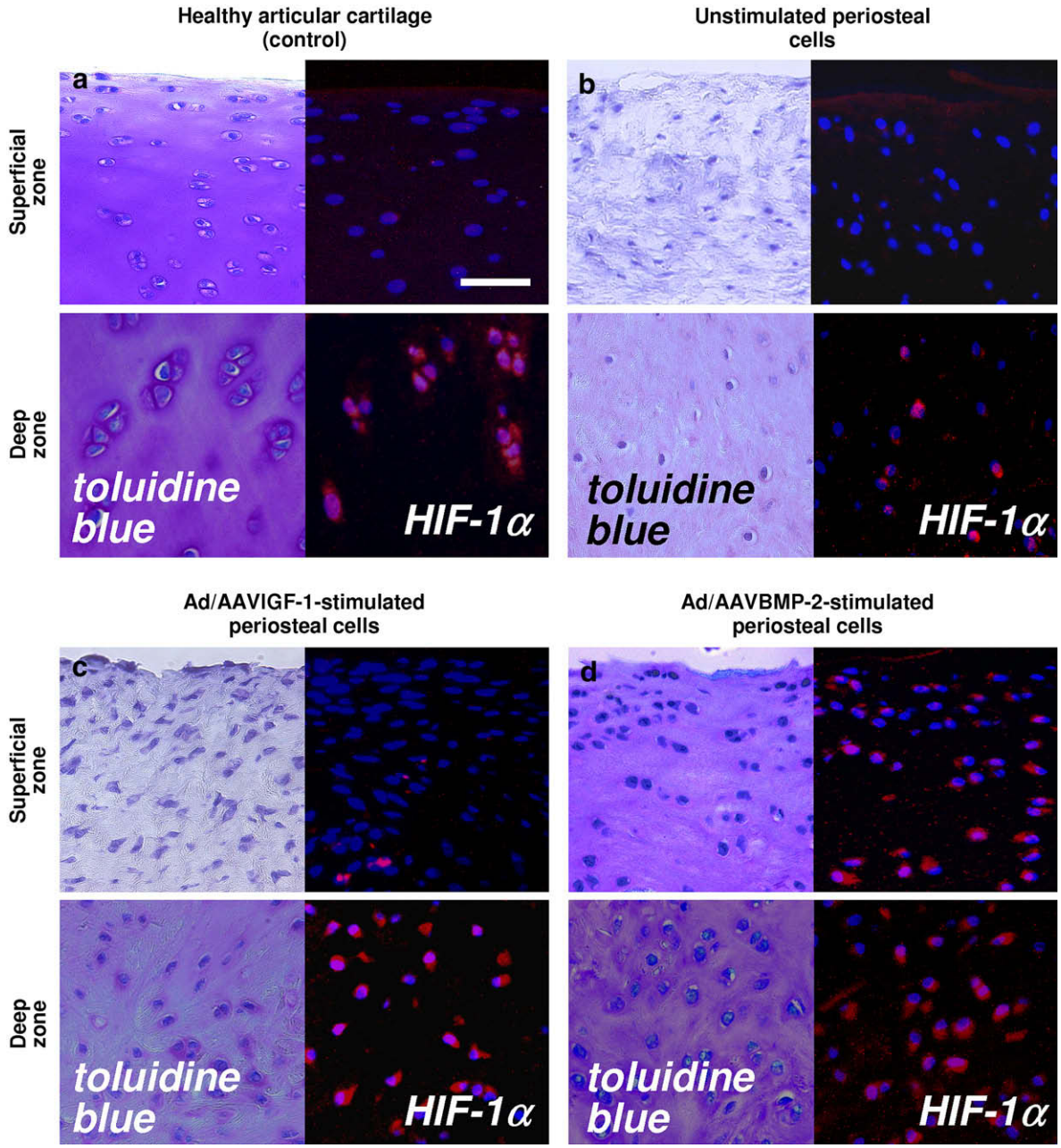

Fig. 4. Zonal differences in cellular morphology and HIF-1α immunostaining (red). Healthy cartilage is characterized by a homogeneous proteoglycan-rich matrix and strong intracellular HIF-1α levels particularly in the deep zones (a). Unstimulated periosteal cells adopted predominantly a spindle-cell like phenotype with no HIF-1α staining in the superficial zone and partial staining in the deepest layer (b). Tissue generated by Ad/AAVIGF-1-stimulated cells was characterized by high cellularity. Only the cells in the deep zones which were surrounded by a proteoglycan-rich pericellular matrix showed HIF-1α staining, while the superficial fibroblast-like cells were negative (c). Ad/AAVBMP-2-stimulated cells adopted a round chondrocyte-like phenotype throughout all layers with mostly strong HIF-1α signals (d). Bar = 50 μm.

of hyaline-like cartilage in deeper zones[22,23]. Our own data have confirmed this tendency. The oxygen distribution pattern may help to explain this phenomenon, since particularly the deepest zones are assumed to be exposed to more hypoxic conditions, provided that the subchondral bone plate remains intact or has been reconstituted. Numerous *in vitro*-studies have shown that low partial pressures of oxygen are involved in promoting the chondrogenic differentiation process[9,10,12,24]. A recent study on full-thickness cartilage defects in miniature pigs also demonstrated the beneficial effect of a functional barrier toward the vascularized bone marrow by using an anti-angiogenic substance[25].

One of the most important factors associated with low oxygen tensions is the transcription factor HIF-1. Although HIF-1 is known to have multiple functions in many tissues, its role in the avascular cartilage and in embryonal mesenchymal condensations is of great importance. HIF-1 was shown to transactivate Sox9, a key factor for the expression of numerous cartilage-specific genes, in mesenchymal cells[12]. A recent study demonstrated direct binding of the

Table II
*Percentage of HIF-1α-positive cells in the superficial half and the deep half of the respective repair tissues and healthy articular cartilage. Three independent superficial and deep areas per specimen were investigated. *P < 0.05, ***P < 0.001 (versus unstimulated repair tissue)*

Tissue	Zone	% of HIF-1α-positive cells
Healthy articular cartilage	Superficial	4.9 (±3.9)
	Deep	92.8* (±6.0)
Unstimulated repair tissue	Superficial	0.8 (±0.3)
	Deep	42.0 (± 7.5)
Ad/AAVIGF-1-stimulated repair tissue	Superficial	3.1* (±1.2)
	Deep	55.9 (±9.0)
Ad/AAVBMP-2-stimulated repair tissue	Superficial	53.2*** (±8.2)
	Deep	74.5* (±9.0)

HIF-1 subunit HIF-1α to the Sox9 promotor region[26]. Furthermore, targeted deletion of HIF-1α in stromal or prechondrogenic cells specifically compromised chondrogenesis while osteogenesis and adipogenesis were not affected[16,26].

Our study is the first to show *in vivo* that the expression of HIF-1α correlates with the quality of a cartilage repair tissue. Furthermore, we could demonstrate that the beneficial effects of BMP-2 on inducing chondrogenesis in the repair tissue were associated with increased HIF-1α expression.

In our experiments *in vitro* using periosteal cells, HIF-1α protein levels could also be increased by stimulation with IGF-1, which confirms the data from previous studies on other cell types including retinal pigment epithelial cells and colon cancer cells[27,28]. The minor effects of IGF-1 on HIF-1α levels in the repair tissue of our *in vivo*-model may be explained by a dose-dependence that was also observed *in vitro*. Thus, the IGF-1 quantities provided by gene transfer and subsequent cell transplantation *in vivo* did presumably not reach the levels that were shown to be required *in vitro*. Consequently, IGF-1 may have a lower potency on increasing intracellular HIF-1α levels compared with BMP-2.

Another aim of this study was to investigate the mechanisms by which growth- or differentiation factors such as IGF-1 or BMP-2 may lead to an increase of HIF-1α expression. In principal, increased protein levels can be achieved *via* enhanced gene expression or translation or by stabilization of mRNA or protein by inhibition of their degradation. In our experiments, neither BMP-2 nor IGF-1 had a direct influence on HIF-1α gene expression. This confirms recent observations made on other cell types, in which IGF-1 had no effect on HIF-1α mRNA synthesis either[27,28].

Probably the most important pathway regulating HIF-1 is the modulation of degradation of its HIFα subunits, which is predominantly mediated by the oxygen-dependent PHD2. However, in our experiments *in vitro*, neither IGF-1 nor

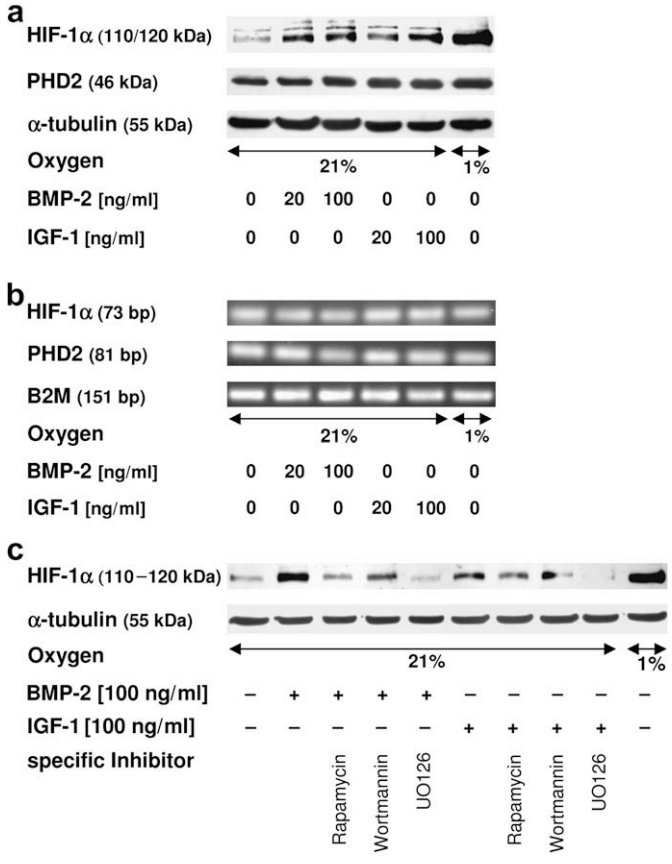

Fig. 5. (a) Induction of HIF-1α by administration of BMP-2 or IGF-1 or cell cultivation under hypoxia. Periosteal cells were stimulated with increasing concentrations of BMP-2 or IGF-1. Nuclear protein extracts were analyzed for HIF-1α protein, and whole cell lysates were collected for PHD2 protein detection by Western blotting. Blots were stripped and re-probed for α-tubulin. (b) BMP-2, IGF-1 and hypoxia have no effect on the expression of HIF-1α and PHD2. Total RNA extracts from stimulated cells were investigated by RT-PCR for HIF-1α and PHD2 gene expression. Detection of B2M expression served as an internal control. (c) HIF-1α induction by BMP-2 or IGF-1 administration was moderately decreased by Wortmannin (PI3K inhibitor) and Rapamycin (mTOR inhibitor), but nearly completely abolished by UO126 (MEK inhibitor). All blots and gels are representative results of three independent experiments.

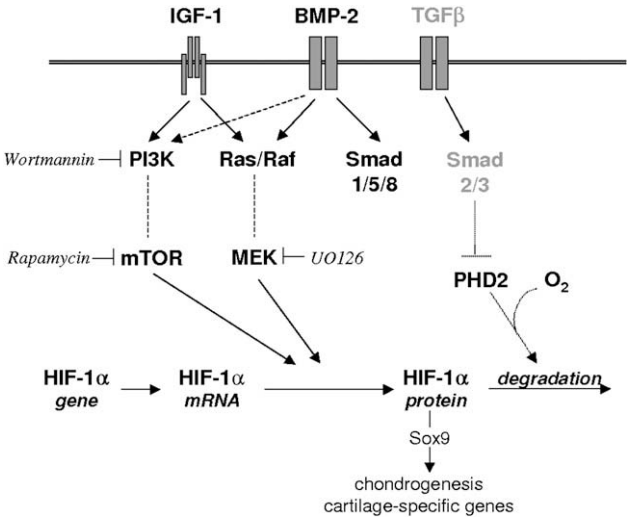

Fig. 6. Proposed functional relationship between different chondrogenic growth- or differentiation factors and HIF-1α, which was recently shown to transactivate Sox9, a key transcription factor for a number of cartilage-specific genes. BMP-2 signaling does not only involve the Smad1/5/8 cascade, but similar to IGF-1 also the PI3K/mTOR and the MEK/ERK pathway. Particularly UO126, a MEK inhibitor, nearly completely abolished HIF-1α induction by BMP-2 or IGF-1. Inhibition of PI3K by Wortmannin and inhibition of mTOR by Rapamycin affected the HIF-1α levels only moderately. Neither IGF-1 nor BMP-2 had any effect on the HIF-1α or PHD2 gene expression. This stands in contrast to the effects of TGFβ which was shown to inhibit PHD2 gene expression *via* Smad2/3.

BMP-2 interferred with the gene expression or protein level of PHD2. Thus the effects of IGF-1 and BMP-2 are unlikely to be mediated by an influence on the stability of the HIF-1α protein either. As far as IGF-1 is concerned, these observations have already been confirmed in studies on other cell types. Those studies suggested that IGF-1 increases HIF-1α protein levels through a posttranscriptional mechanism involving the PI3K/mTOR and the MEK/ERK pathways without modulating HIF-1α transcription but by stimulation of its translation[27,28,29]. We could confirm this effect also for periosteal cells. The increase of HIF-1α levels subsequent to an IGF-1 stimulus is mediated predominantly *via* the MEK/ERK pathway and to a lesser extent *via* the PI3K/mTOR pathway.

To date, no data on interactive mechanisms between BMP-2 and increased HIF-1α levels have been published. In fact, it has been shown that the functionally related transforming growth factor-β (TGFβ) stabilizes HIF-1α protein by inhibiting the expression of PHD2 and thus inhibiting HIF-1α degradation *via* a cascade involving Smad2/3 signaling[30]. However, in our experiments, BMP-2 had no influence on the expression of PHD2 or PHD3 (K. Gelse, unpublished data). This may be based on the fact that, in contrast to TGFβ signaling, BMP-2 involves the Smad1/5/8 cascade rather than the Smad2/3 cascade[31], which may explain the different effects of TGFβ and BMP-2 on PHD2 expression.

There is good evidence that, intracellulary, BMP signals are not only transduced by the Smad pathway but also by the PI3K/mTOR and mitogen-activated protein (MAP)-kinase cascades[32,33]. In this study, the inhibiton of MEK by UO126 almost completely abolished HIF-1α induction following BMP-2 stimulation, indicating that the MEK/ERK pathway plays an important role in increasing the levels of HIF-1α. The inhibiton of PI3K and mTOR by Wortmannin or Rapamycin, respectively, had only a moderate effect. Future studies will have to investigate the role of the Smad1/5/8 signaling in this respect.

As the conclusions of this study are weakened by the relatively small number of animals, further work on larger groups of animals is required, including the additional use of other cells types such as committed chondrocytes. Nevertheless, the data of this pilot experimental work contribute new aspects to the knowledge about pro-chondrogenic signaling pathways as summarized in Fig. 6, supporting the conclusion that growth factors of different families may use common as well as distinct pathways to exert their stimulatory effects on chondrogenesis.

In many experimental studies, chondroinductive differentiation factors such as BMPs have been shown to stimulate efficiently the formation of hyaline-like repair tissue. However, the clinical use of such factors may be limited by tremendous costs arising from the administration of recombinant proteins, and gene transfer approaches may be hindered because of safety concerns. Therefore, the association of HIF-1α with chondrogenic pathways may be particularly interesting. Although, the interactions between hypoxia, HIF-1α and chondrogenic pathways will have to be explored in detail in future, our findings may encourage the establishment of new cartilage repair strategies that incorporate the potential beneficial role of low oxygen and/or elevated HIF-1α levels as a therapeutic tool for cartilage repair.

Conflict of interest

All authors disclose any financial and personal relationships with other people or organizations that could inappropriately influence (bias) this work, including employment, consultancies, stock ownership, honoraria, paid expert testimony, patent applications/registrations, and grants or other funding.

Acknowledgements

We thank E. Koppmann, M. Geßlein and H. Rohrmüller for excellent technical assistance, Dr Philippe Moullier (Genethon, Nantes, France) for providing the plasmid pRepCap, Dr Richard Samulski (University of North Carolina, USA) for the plasmid pXX6-80, and Geistlich Biomaterials (Wolhusen, Switzerland) for the Chondrogide membranes. Supported by the Interdisciplinary Center of Clinical Research (IZKF) at the University Hospital Erlangen (grants C1 and C7) and the German Research Foundation (grant GE 1975/1-2).

Supplementary data

Supplementary material associated with this article can be found, in the online version, at doi:10.1016/j.joca.2008.04.006.

References

1. Winter A, Breit S, Parsch D, Benz K, Steck E, Hauner H, *et al.* Cartilage-like gene expression in differentiated human stem cell spheroids: a comparison of bone marrow-derived and adipose tissue-derived stromal cells. Arthritis Rheum 2003;48:418–29.
2. Park J, Gelse K, Frank S, von der Mark K, Aigner T, Schneider H. Transgene-activated mesenchymal cells for articular cartilage repair: a comparison of primary bone marrow-, perichondrium/periosteum- and fat-derived cells. J Gene Med 2006;8:112–25.

3. De Bari C, Dell'Accio F, Tylzanowski P, Luyten FP. Multipotent mesenchymal stem cells from adult human synovial membrane. Arthritis Rheum 2001;44:1928–42.
4. Gelse K, Jiang QJ, Aigner T, Ritter T, Wagner K, Poschl E, *et al*. Fibroblast-mediated delivery of growth factor complementary DNA into mouse joints induces chondrogenesis but avoids the disadvantages of direct viral gene transfer. Arthritis Rheum 2001;44:1943–53.
5. Adachi N, Sato K, Usas A, Fu FH, Ochi M, Han CW, *et al*. Muscle derived, cell based *ex vivo* gene therapy for treatment of full thickness articular cartilage defects. J Rheumatol 2002;29:1920–30.
6. De Bari C, Dell'Accio F, Luyten FP. Human periosteum-derived cells maintain phenotypic stability and chondrogenic potential throughout expansion regardless of donor age. Arthritis Rheum 2001;44:85–95.
7. De Bari C, Dell'Accio F, Vanlauwe J, Eyckmans J, Khan IM, Archer CW, *et al*. Mesenchymal multipotency of adult human periosteal cells demonstrated by single-cell lineage analysis. Arthritis Rheum 2006;54:1209–21.
8. Silver IA. Measurement of pH and ionic composition of pericellular sites. Philos Trans R Soc Lond B Biol Sci 1975;271:261–72.
9. Hirao M, Tamai N, Tsumaki N, Yoshikawa H, Myoui A. Oxygen tension regulates chondrocyte differentiation and function during endochondral ossification. J Biol Chem 2006;281:31079–92.
10. Kurz B, Domm C, Jin M, Sellckau R, Schunke M. Tissue engineering of articular cartilage under the influence of collagen I/III membranes and low oxygen tension. Tissue Eng 2004;10:1277–86.
11. Pfander D, Cramer T, Schipani E, Johnson RS. HIF-1alpha controls extracellular matrix synthesis by epiphyseal chondrocytes. J Cell Sci 2003;116:1819–26.
12. Robins JC, Akeno N, Mukherjee A, Dalal RR, Aronow BJ, Koopman P, *et al*. Hypoxia induces chondrocyte-specific gene expression in mesenchymal cells in association with transcriptional activation of Sox9. Bone 2005;37:313–22.
13. Schipani E, Ryan HE, Didrickson S, Kobayashi T, Knight M, Johnson RS. Hypoxia in cartilage: HIF-1alpha is essential for chondrocyte growth arrest and survival. Genes Dev 2001;15:2865–76.
14. Maxwell PH, Ratcliffe PJ. Oxygen sensors and angiogenesis. Semin Cell Dev Biol 2002;13:29–37.
15. Provot S, Zinyk D, Gunes Y, Kathri R, Le Q, Kronenberg HM, *et al*. Hif-1alpha regulates differentiation of limb bud mesenchyme and joint development. J Cell Biol 2007;177:451–64.
16. Malladi P, Xu Y, Chiou M, Giaccia AJ, Longaker MT. Hypoxia inducible factor-1alpha deficiency affects chondrogenesis of adipose-derived adult stromal cells. Tissue Eng 2007;13:1159–71.
17. Berra E, Benizri E, Ginouves A, Volmat V, Roux D, Pouyssegur J. HIF prolyl-hydroxylase 2 is the key oxygen sensor setting low steady-state levels of HIF-1alpha in normoxia. EMBO J 2003;22:4082–90.
18. Xiao X, Li J, Samulski RJ. Production of high-titer recombinant adeno-associated virus vectors in the absence of helper adenovirus. J Virol 1998;72:2224–32.
19. Snyder RO, Xiao X, Samulski RJ. Production of recombinant adeno-associated viral vectors. In: Dracpoli N, Haines J, Krof B, Eds. Current Protocols in Human Genetics. New York: Wiley; 1996: 1–24.
20. Gelse K, Muhle C, Franke O, Park J, Jehle M, Durst K, *et al*. Cell-based resurfacing of large cartilage defects: long-term evaluation of grafts from autologous transgene-activated periosteal cells in a porcine model of osteoarthritis. Arthritis Rheum 2008;58:475–88.
21. Grimmer C, Pfander D, Swoboda B, Aigner T, Mueller L, Hennig FF, *et al*. Hypoxia-inducible factor 1alpha is involved in the prostaglandin metabolism of osteoarthritic cartilage through up-regulation of microsomal prostaglandin E synthase 1 in articular chondrocytes. Arthritis Rheum 2007;56:4084–94.
22. Behrens P, Bitter T, Kurz B, Russlies M. Matrix-associated autologous chondrocyte transplantation/implantation (MACT/MACI) – 5-year follow-up. Knee 2006;13:194–202.
23. Knutsen G, Engebretsen L, Ludvigsen TC, Drogset JO, Grontvedt T, Solheim E, *et al*. Autologous chondrocyte implantation compared with microfracture in the knee. A randomized trial. J Bone Joint Surg Am 2004;86-A:455–64.
24. Chen L, Fink T, Ebbesen P, Zachar V. Temporal transcriptome of mouse ATDC5 chondroprogenitors differentiating under hypoxic conditions. Exp Cell Res 2006;312:1727–44.
25. Hunziker EB, Driesang IM. Functional barrier principle for growth-factor-based articular cartilage repair. Osteoarthritis Cartilage 2003;11: 320–7.
26. Amarilio R, Viukov SV, Sharir A, Eshkar-Oren I, Johnson RS, Zelzer E. HIF1{alpha} regulation of Sox9 is necessary to maintain differentiation of hypoxic prechondrogenic cells during early skeletogenesis. Development 2007;134:3917–28.
27. Fukuda R, Hirota K, Fan F, Jung YD, Ellis LM, Semenza GL. Insulin-like growth factor 1 induces hypoxia-inducible factor 1-mediated vascular endothelial growth factor expression, which is dependent on MAP kinase and phosphatidylinositol 3-kinase signaling in colon cancer cells. J Biol Chem 2002;277:38205–11.
28. Treins C, Giorgetti-Peraldi S, Murdaca J, Monthouel-Kartmann MN, Van Obberghen E. Regulation of hypoxia-inducible factor (HIF)-1 activity and expression of HIF hydroxylases in response to insulin-like growth factor I. Mol Endocrinol 2005;19:1304–17.
29. Catrina SB, Botusan IR, Rantanen A, Catrina AI, Pyakurel P, Savu O, *et al*. Hypoxia-inducible factor-1alpha and hypoxia-inducible factor-2alpha are expressed in kaposi sarcoma and modulated by insulin-like growth factor-I. Clin Cancer Res 2006;12:4506–14.
30. McMahon S, Charbonneau M, Grandmont S, Richard DE, Dubois CM. Transforming growth factor beta1 induces hypoxia-inducible factor-1 stabilization through selective inhibition of PHD2 expression. J Biol Chem 2006;281:24171–81.
31. Wan M, Cao X. BMP signaling in skeletal development. Biochem Biophys Res Commun 2005;328:651–7.
32. Langenfeld EM, Kong Y, Langenfeld J. Bone morphogenetic protein-2-induced transformation involves the activation of mammalian target of rapamycin. Mol Cancer Res 2005;3:679–84.
33. Zhao M, Xiao G, Berry JE, Franceschi RT, Reddi A, Somerman MJ. Bone morphogenetic protein 2 induces dental follicle cells to differentiate toward a cementoblast/osteoblast phenotype. J Bone Miner Res 2002;17:1441–51.